One-Step Deblurring and Denoising Color Images Using Partial Differential Equations

Danny Barash[1]
HP Laboratories Israel
HPL-2000-102 (R.1)
January 19th, 2001*

email: barash@hpli.hpl.hp.com

nonlinear diffusion filtering, deblurring, denoising

An implicit, one-step method for the restoration of blurred and noisy color images is presented. Using a nonlinear partial differential equation (PDE)-based variational restoration approach, it is shown that a single iteration yields a result that is visually superior to performing Gaussian low-pass filtering, followed up by unsharp masking, a conventional linear process. The governing equation is constructed by examining ways to achieve the optimal balance between the two competitive forces, that of denoising and deblurring, at the same time. For the solution, the additive operator splitting (AOS) scheme is implemented, which allows the separation of spatial variables. A stable and efficient algorithm results from the decomposition of the problem, that has recently been developed for denoising without deblurring. Deblurring is added to denoising in such a way that the tridiagonal structure in each one of the dimensions is preserved, so that the algorithm remains inexpensive despite the matrix inversions. Results indicate that this one-step implementation yields a robust filter that can be tuned to preprocess images for various applications.

* Internal Accession Date Only
Approved for External Publication
[1] HP Labs – Israel, Technion City, Haifa 32000, Israel

1 Introduction

Nonlinear variational image restoration methods have recently gained much interest in image processing. The success of the Total Variation (TV) norm in noise removal [9] and image reconstruction, as well as related pioneering work on nonlinear diffusion filters [8, 12], has led to the development of efficient methods [13] for solving the governing PDE. These methods can potentially be used in numerous applications, tackling important problems in the areas of image processing, analysis and computer vision.

One such traditional problem in image restoration is that of reconstructing a blurred and noisy image, in which the resultant image should faithfully represent the original. Some related past efforts can be found in [6, 3, 2, 11, 7]. Here the motivation is to apply a fast and efficient method, based on nonlinear variational formulation and PDEs, to perform denoising and deblurring in a singe large time step. The result is shown to be superior to successively using a low pass-filter for the denoising, and unsharp masking for the deblurring, both operating linearly on the image to produce a fast result. By using an efficient method, the speed and complexity of the nonlinear approach to the problem is not far from the linear case. By decomposing the problem, which comes naturally when using the additive operator splitting (AOS) proposed in [13], it is also simpler to understand the effect of nonlinearities in the governing equation on the restoration process by examining one-dimensional cross-sections of the image.

The paper is divided as follows. Section 2 describes the problem formulation, starting from an energy functional to be minimized. The Euler-Lagrange equation resulting from this formulation is presented. In Section 3, numerical schemes are discussed for the solution of the governing PDE. Section 4 presents the solution of the approach which was built in the previous two sections, processing three color test images, and comparing the results of different regularizations and a conventional simple linear solution. Section 5 attempts to understand the nonlinear processing that was performed, by examining one-dimensional slices of the image. Section 6 concludes this work.

2 Problem Formulation

Let us assume that during an image acquisition stage, the original image is blurred by a known point-spread function (PSF) and subsequently noise is added. The image degradation model is of the form

$$f(x, y) = (d * u)(x, y) + n(x, y) \tag{1}$$

where $u(x, y)$ is the desired original image, d is the known blur PSF, $*$ denotes the two-dimensional convolution, f is the observed degraded image, and n denotes the additive noise that is present in that image.

Our goal is to reconstruct u from f. In order to optimally perform the reconstruction, we would like to minimize some kind of image norm that measures the degree of smoothness, denoted by $\psi(|\nabla u|^2)$, where ψ is called the smoothness potential

$$\min_{u(x,y)} \int_{\Omega} \psi(|\nabla u(x,y)|^2)\, dx\, dy, \tag{2}$$

subject to the constraint

$$\int_{\Omega} (d * u - f)^2\, dx\, dy = \sigma^2, \tag{3}$$

where without loss of generality a unit support for the image is assumed ($|\Omega| = 1$), $x, y \in \Omega$ and σ is the noise standard deviation. The constraint is responsible for keeping the estimated image u close to the initial degraded image f. Instead of the minimization with a constraint in Equations (2),(3), the problem can be formulated as that of minimizing the energy functional

$$\min_{u} \int_{\Omega} \psi(|\nabla u|^2) + \alpha(d * u - f)^2\, dx\, dy \tag{4}$$

where α is a Lagrange-multiplier. Using calculus of variations, equation (4) satisfies the Euler-Lagrange equation

$$0 = \nabla \cdot (\psi\prime(|\nabla u|^2)\nabla u) + \alpha d * (d * u - f) \tag{5}$$

where $\psi\prime$ is the derivative of ψ. There are several methods for the solution of (5), see for example [2, 11]. Moreover, one can solve (5) in a time-dependent framework, by advancing the following PDE to its steady-state ($t \to \infty$) solution

$$\frac{\partial u}{\partial t} = \nabla \cdot (\psi\prime(|\nabla u|^2)\nabla u) + \alpha d * (d * u - f) \tag{6}$$

The choice of an appropriate ψ is important, since the quality of the result is sensitive to $\psi\prime$, the diffusivity term. For denoising, the total variation smoothness potential $\psi(|\nabla u|^2) = |\nabla u|$ was used in [9], whereas in [14] a convex smoothing potential of the form $\psi(|\nabla u|^2) = \lambda\sqrt{1 + |\nabla u|^2/\lambda^2} + \varepsilon|\nabla u|^2$, $(\lambda, \varepsilon > 0)$, is applied. The latter potential is a generalization of the former. In reference [6], the latter potential with $\varepsilon = 0$ is chosen, which amounts to a total variation potential. Common to our work, that paper attempts to solve equation (6) numerically. However, unlike several iterations of an explicit algorithm, we take a different approach in trying to approximate the solution to (6) by using one iteration with an implicit method. In [1], several other possibilities for a smoothing potential are explored in the context of anisotropic diffusion filtering, all of which are motivated by the analogy to robust estimation. A related work on the connection between variational image restoration and diffusion filtering [10] examines some theoretical aspects of these potentials.

After experimenting with many of these smoothing potentials, a particular version of the regularized Perona-Malik filter [8, 10] is chosen for the rest of this paper. The corresponding smoothing potential is of the form $\psi(|\nabla u|^2) = \ln(1 + |\nabla L_\sigma u|^2)$ for the filter's fullest version, where L_σ is a convolution operator with a smooth kernel. The regularized Perona-Malik filter was recently revived in [10] where its well-posedness and convergence characteristics were studied. The justification for using this particular potential in our case for denoising and deblurring is the notion of backward diffusion, that can be traced back to Perona and Malik's original paper [8]. By allowing backward diffusion, it is possible to achieve edge-enhancement along with edge-preserving smoothing. We will elaborate more on some other possible choices of smoothing potentials in Section 4.

Choosing one particular type of a regularized Perona-Malik filter, equation (6) becomes

$$\frac{\partial u}{\partial t} = \nabla \cdot \left(\frac{1}{1 + |\nabla L_\sigma u|^2 / c} \nabla u \right) + \alpha d * (d * u - f) \tag{7}$$

where $c = 1.0$ was chosen for our calculations. The regularization operation, $L_\sigma u$, is a presmoothing mechanism in which the image u is convolved with a Gaussian of standard deviation σ, the regularization parameter.

3 Implementation

This section describes the numerical scheme that we use to solve (7) efficiently. It starts from the one-dimensional semi-implicit scheme, which will be applied for the analysis in Section 5, and then builds upon the one-dimensional scheme to describe the two-dimensional scheme that is implemented for processing the noisy blurred images in Section 4. More details about the schemes can be found in [13], where they were originally proposed. Here, the AOS scheme is implemented on a problem with a certain constraint. Examples for the implementation of the AOS scheme on other type of constraints can be found in [4, 14].

First, let us review the derivation of the one-dimensional semi-implicit scheme. A simple discretization for solving the anisotropic diffusion equation, an equation similar to (7), can be written using a compact matrix notation as proposed in [13]. First, the nonlinear spatial term is discretized by

$$\nabla \cdot (g(|\nabla u|^2) \nabla u) = \sum_{j \in \mathcal{N}(\mathrm{i})} \frac{g_j^k + g_i^k}{2h^2} (u_j^k - u_i^k) \tag{8}$$

where $\mathcal{N}(\mathrm{i})$ is the set of two neighbors of i, one neighbor for the boundary pixels. It follows that equation (7) can now be discretized in full, and a compact way of writing this discretization is

$$\frac{u^{k+1} - u^k}{\tau} = A(u^k) u^k + \alpha d * (d * u^k - f^k), \tag{9}$$

where u^k is a signal vector of size N and $A(u^k) = (a_{ij}(u^k))$ is an $N \times N$ matrix whose elements are given by

$$a_{ij}(u^k) = \begin{cases} \frac{g_i^k + g_j^k}{2h^2} & j \in \mathcal{N}(\mathrm{i}), \\ -\sum_{n \in \mathcal{N}(\mathrm{i})} \frac{g_i^k + g_n^k}{2h^2} & j = i, \\ 0 & \text{otherwise.} \end{cases} \tag{10}$$

Isolating u^{k+1} on the left hand side, we obtain

$$u^{k+1} = (I + \tau A(u^k))u^k + \alpha d * (d * u^k - f^k). \tag{11}$$

This scheme is known as the *explicit scheme*, since u^{k+1} is obtained explicitly from u^k without a matrix inversion. This scheme, that is based on forward Euler [5], is simple, straight-forward, and computationally cheap because only matrix-vector multiplications are required. However, it is conditionally stable and therefore limited to small time steps. A similar scheme was also used in [6], and requires several iterations with small time steps because of the stability constraint. Our goal is to implement (7) with the fewest number of iterations as possible, preferably even a single iteration. In order to use a single large time step, we explore another scheme that was proposed in [13], which is based on backward Euler

$$\frac{u^{k+1} - u^k}{\tau} = A(u^k)u^{k+1} + \alpha d * (d * u^k - f^k), \tag{12}$$

Rearranging terms, so that u^{k+1} is on the left hand side and u^k is on the right hand side, we obtain

$$(I - \tau A(u^k))u^{k+1} = u^k + \alpha d * (d * u^k - f^k). \tag{13}$$

This scheme is known as the *semi-implicit scheme*, since u^{k+1} is obtained implicitly from u^k by inverting a matrix. Although a matrix inversion is in general an expensive $O(N^3)$ operation, the matrix in equation (13) is a tridiagonal matrix which can be inverted efficiently with a complexity of $O(N)$. The semi-implicit scheme is unconditionally stable, with no constraints on the time step due to stability considerations. A straight-forward extension of the one-dimensional semi-implicit scheme (13) to higher dimensions is

$$\left(I - \tau \sum_{l=1}^{m} A_l(u^k)\right) u^{k+1} = u^k + \alpha d * (d * u^k - f^k), \tag{14}$$

where m is the number of coordinates. The matrix $A_l(u^k)$ corresponds to the derivatives along the l-th coordinate axis. The scheme is again unconditionally stable. It is worthwhile noticing that the only drawback when moving to higher dimensions is in the efficiency of (14): the matrix $\sum_{l=1}^{m} A_l(u^k)$ is no longer tridiagonal and therefore the matrix inversion at each time step is costly. Therefore, split-operator methods [5] are proposed for gaining efficiency

by the concept of separation of variables. The operator splitting scheme proposed in [13] as the method of choice, the *additive operator splitting* (AOS), is

$$\frac{1}{m}\sum_{l=1}^{m}\left(I - m\tau A_l(u^k)\right)u^{k+1} = u^k + \alpha d * (d * u^k - f^k). \tag{15}$$

The scheme in (15) is unconditionally stable, reliable and efficient, and will be used for solving (7) numerically. Moreover, the results are obtained with a single time step of $\Delta t = 10.0$, which means that only two tridiagonal matrix inversions are enough to get to a point near the optimum of the functional in (4) that is visually satisfactory. For the blurring d, in all our experiments we first construct the matrix D:

$$D = \begin{cases} 0.5 & \text{if } i = j \\ 0.25 & \text{if } |i-j| = 1, \text{ or } (i,j) = (1,N),\ (N,1) \\ 0 & \text{otherwise} \end{cases} \tag{16}$$

where the matrix is of size $N \times N$, corresponding to a square image. For an image U, $d * U$ is equivalent to DUD^T. We assume that the noise is an additive random noise with a variance of $\sigma^2 = 6.0$, with zero mean. Finally, the regularization step for calculating the presmoothing operation $L_\sigma u$ in (7), is done by solving the linear diffusion equation for a very small time step of size $T = \sigma^2/2$ before each iteration. Since the equation is linear, a simpler splitting scheme than the AOS can be used for the regularization step. We chose the locally one-dimensional (LOD) scheme, described in [13], for the implementation of the regularization step in our experiments.

4 Results

Figure 1 presents an original color image which is used to test our algorithm. After blurring and adding noise to the original image by using the parameter values specified in Section 3, we reach the degraded image observed in Figure 2. A straight-forward method to approximate the original image, starting from the degraded image, is to apply a median filter for the denoising and then use unsharp masking for the deblurring. Experimenting with several parameter values to find the best combination, we reach the restored image in Figure 3.

The variational nonlinear restoration approach, described in the previous sections, can now be applied to improve the degraded image in Figure 2. We note that throughout this work, we remain in RGB color space treating each channel independently. In order to add a perceptual component to our model, let us propose a slight modification that takes into account the fact that the human eye tends to prefer sharp images. Instead of the constraint in (3), keeping the image u close to the initial degraded image f, let us keep the image u close to a deblurred initial image $d^{-1} * f$. Our initial condition remains the image f. As a consequence, the resulting Euler-Lagrange equation is slightly modified compared to equation (7). It now

becomes

$$\frac{\partial u}{\partial t} = \nabla \cdot \left(\frac{1}{1 + |\nabla L_\sigma u|^2 / c} \nabla u \right) + \alpha (d * d * u - f). \tag{17}$$

Since $d * d^{-1} * f = f$. The term associated with the parameter α is responsible for the deblurring. Figures 4,5 illustrate the difference between applying equations (7),(17) respectively, after tuning each of the two for best restoration of our reference test image. We will see that in Table 1, where quantitative (non-visual) comparison of the amount of closeness to the original image in Figure 1 is performed, the modification done in equation (17) actually causes a larger deviation from the original, as expected. However, qualitative visual examination of Figure 5 reveals a somewhat shaper looking image compared to Figure 4 (it is sometimes difficult to observe this effect on a printed paper, an image viewer can highlight the difference). Our experiments on the other test images indicate that this way of introducing extra sharpening before the tuning can produce some visually more pleasing results with no extra effort. As long as we anticipate its effect, this modification is sound and within the general framework of our model.

Using the one step implicit method to approximate the solution to (17), we try different values for the regularization parameter σ. As expected, zero regularization produces an over-sharpened image, as in Figure 6, whereas $\sigma = 0.5$ generates an image that is too smooth (see Figure 7). The right balance is achieved with a regularization of $\sigma = 0.25$, as in Figure 5, which is closer to the original image in Figure 1 than the attempt in Figure 3.

The solution method applied to approximate (17) uses a single iteration of $\Delta t = 10.0$ with an implicit method. We note that performing 10 iterations of $\Delta t = 0.1$, has a minor effect on the resultant image. In addition, applying the explicit Forward-Euler instead of the implicit Backward-Euler does not succeed to get far from the initial degraded image in a single time step. This is expected, since the diffusion equation has an infinite propagation speed [5]. The Backward-Euler has an infinite numerical signal propagation speed, i.e. information propagates throughout the entire physical space during each time step. The Forward-Euler has only a finite numerical propagation speed, therefore its performance is substantially limited when using a single time step.

The procedure of designing the filter is as follows. It is possible to tune the parameters once, using a natural test image. Then, different diffusivity functions $g(|\nabla u|^2)$ can be picked, along with adapting the threshold as desired. We note that the regularized Perona-Malik discussed in Section 2 is relatively insensitive to the threshold - a single threshold can be used for all subsequent images. If we use the CLMC filter (see [13]), more smoothing can be achieved on flat regions but the noise is not distributed evenly over the whole image as a consequence. When we use the convex smoothing potential [14], it is possible to achieve evenly distributed noise but the image remains noisier. This is somewhat similar to the behavior analyzed in [14]. The regularized Perona-Malik is a good compromise between the

two for the purpose of obtaining an initial satisfactory deblurred and denoised image, but further performance improvements and diffusivity choices depend on the application at hand.

Finally, Figures 8,9,10,11,12,13 apply (17) to improve two other test images which were degraded using the same model described in Section 3. The same parameters that were tuned for the previous test image are used with the new images as well.

Table II: l_2 norm deviation from original			
Image	Initial	Output (17)	Output (7)
Grapes	0.371	0.304	0.300
Packard	0.725	0.686	0.667
Circles	1.463	1.441	1.398

In Table II, the relative l_2 norm deviations are calculated for the three test images. The calculation is performed as follows. Let v denote the original image before the degradation. Let u denote the approximate restoration result. The relative error percentages are calculated by

$$\frac{\|u - v\|_2}{\|v\|_2}. \tag{18}$$

The deviation results are expected from our model. As mentioned earlier, the deviations of Output (7) are smaller than the ones of Output (17). In both cases, an improvement in the deviation from the original is achieved due to the filtering operation, compared to the initial deviation of the degraded image from the original. In the next section, we will try to further understand our output results by analyzing the 1D constituents of our model.

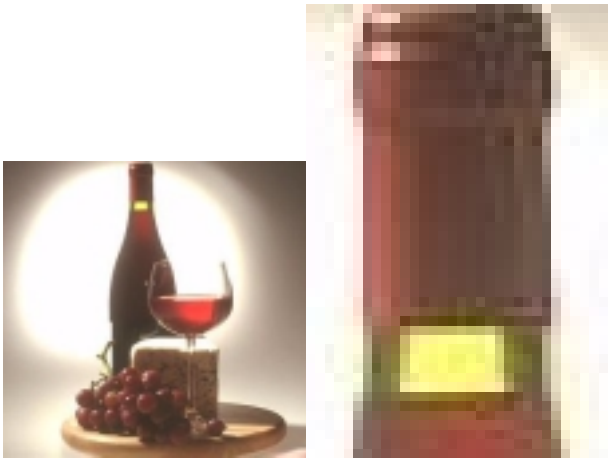

Figure 1: Original image.

Figure 2: Blurred noisy image.

Figure 3: Median with a 3x3 window followed by unsharp masking with 60% enhancement factor.

Figure 4: deblurring and denoising with the one step implicit method according to equation (7), $\alpha = 0.24$, regularization of 0.075.

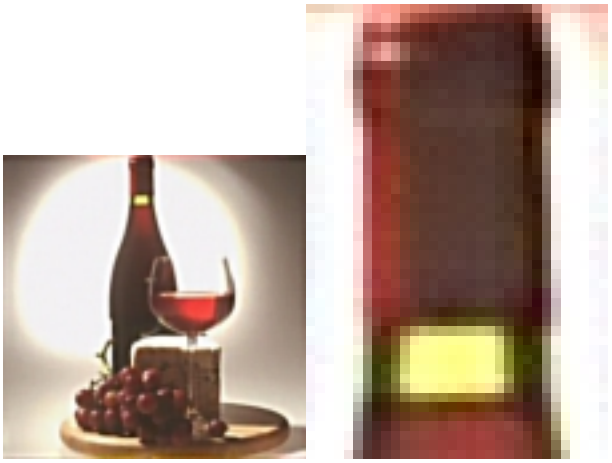

Figure 5: deblurring and denoising with the one step implicit method according to equation (17), $\alpha = 0.08$, regularization of 0.25.

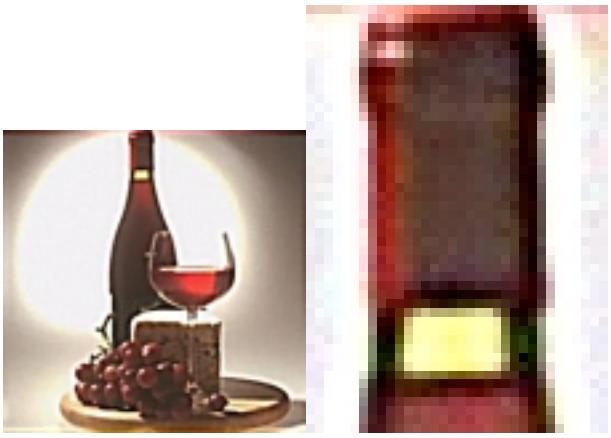

Figure 6: deblurring and denoising with the one step implicit method according to equation (17), no regularization.

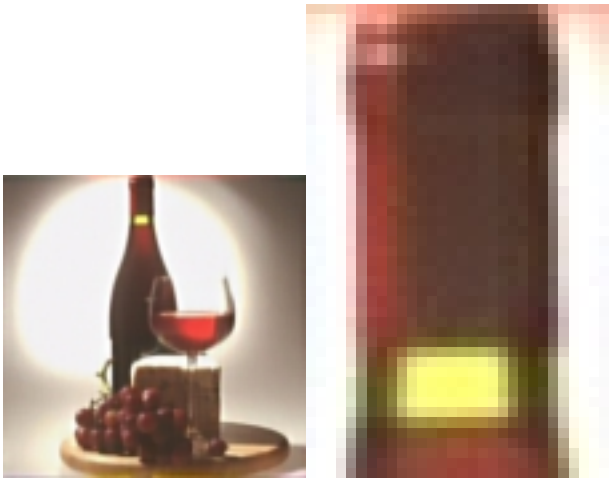

Figure 7: deblurring and denoising with the one step implicit method according to equation (17), regularization of 0.5.

Figure 8: Original image - Packard.

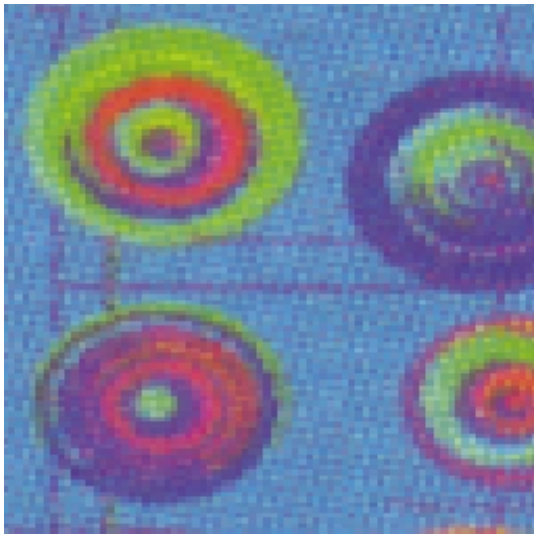

Figure 9: Original image - Circles.

Figure 10: Blurred noisy image - zoom in.

Figure 11: Deblurred and denoised image with the one step implicit method according to equation (17), regularization of 0.25.

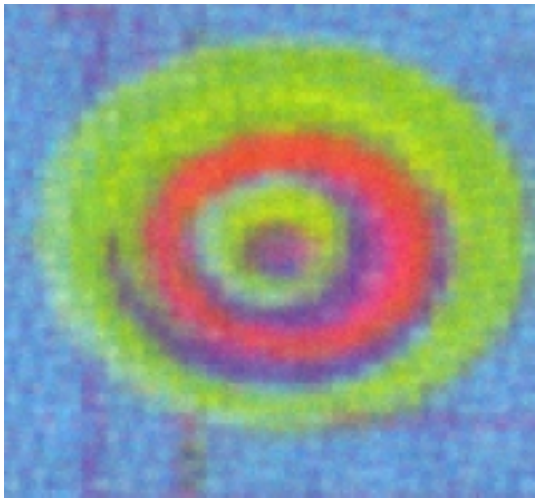

Figure 12: Blurred noisy image - zoom in.

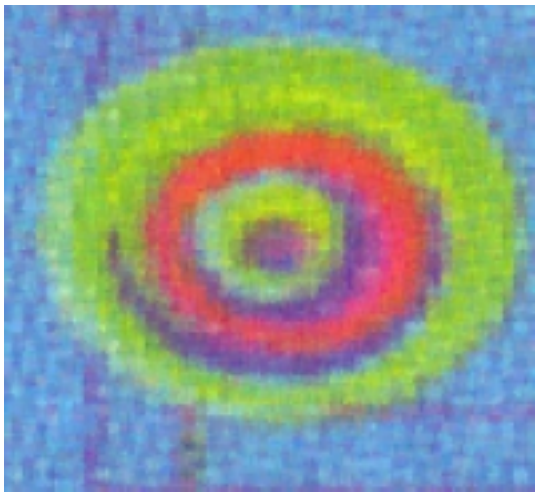

Figure 13: Deblurred and denoised image with the one step implicit method according to equation (17), regularization of 0.25.

5 Analysis

Besides being an efficient scheme, an additional advantage of the AOS scheme is that the 2D scheme consists of 1D building blocks. Therefore, for the analysis, one can easily process 1D slices of the image by using parts of the code that was written for the implementation, or perform an analysis through run-time.

In Figure 14, a one-dimensional horizontal slice of the image that contains the collar of the bottle is plotted, intensity of the red as a function of position. The edge in the middle is clearly visible, both the original edge (Figure 14, left) and the noisy blurred edge (Figure 14, right) are shown.

Although the one-channel (the red) and particular image slice that was chosen can not represent the entire color image in a quantitative manner, their qualitative behavior reveals some important aspects. In Figure 15, it is seen how denoising and deblurring was performed on Figure 14 (right). The one step implicit method result obtained in Figure 15 was able to achieve an edge-sharpening, much like the color image in Figure 5. The method is found to perform the best and achieve the correct trade-off with $\sigma = 0.25$. The two extremes are shown in Figure 10: $\sigma = 0$ results in a strong sharpening of the edge but more noise remains, whereas $\sigma = 0.5$ does the opposite.

Some explanation for the behavior of different smoothing potentials and parameters on the restoration process can be found by examining the nonlinear diffusivity term in our 1D slice. The diffusivity term is dependent on the gradient, where we apply the gradient on the noisy blurred signal of Figure 14 (right). In Figure 17, it is seen how the correct trade-off is achieved: the peak responsible for the edge in the middle of the collar is sharp, and in between the peaks the diffusivity is almost decayed completely. This sharpness surrounding edges is even more pronounced with $\sigma = 0$, Figure 18 (left), but at the expense of increasing the noise. On the contrary, when increasing the regularization to $\sigma = 0.5$, it can be deduced that the edges seen in Figure 16 (right) are less sharp due to the bumps inside the troughs as observed in Figure 18 (right), located in between edges.

6 Conclusions

The problem of deblurring and denoising color images can not be convincingly solved by linear means to produce visually pleasing results, since a correct treatment around edges requires a nonlinear model. In addition, deblurring and denoising are two competing forces that are interfering with each other, which makes the problem even harder. Nonlinear restoration approaches should be used to tackle this problem, but they tend to be computationally expensive and cumbersome.

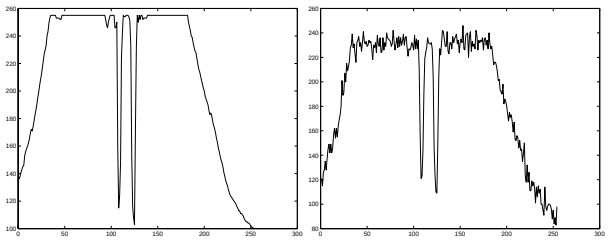

Figure 14: Cross section of the original image and the noisy blurred image.

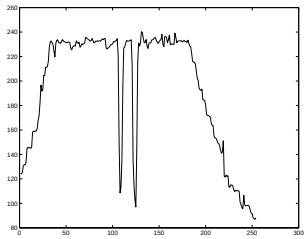

Figure 15: Cross section after processing: one step implicit method with regularization $\sigma = 0.25$.

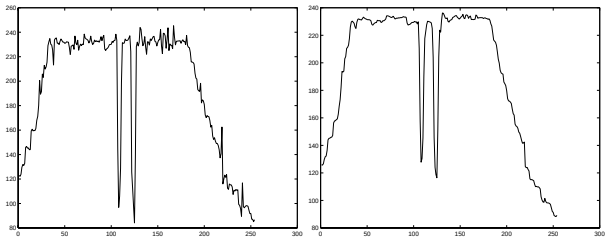

Figure 16: Cross section after processing: one step implicit method with regularizations $\sigma = 0.0$, $\sigma = 0.5$.

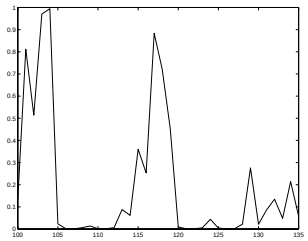

Figure 17: Diffusivity in cross-section: one step implicit method with regularization $\sigma = 0.25$.

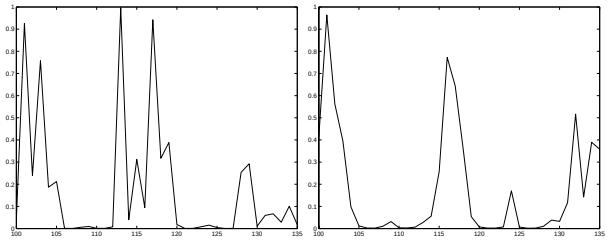

Figure 18: Diffusivity in cross-section: one step implicit method with regularizations $\sigma = 0.0$, $\sigma = 0.5$.

A nonlinear variational restoration approach is proposed which is an extension to recently developed methods for the problem of denoising. The method that results from this approach is fast and efficient, and in a single iteration it is possible to achieve visually pleasing results. Iterative methods may reach closer to the minimum of the functional at hand, but the one-step method might be considered a good trade-off between performance and expense of computation for some applications. It can also be used as a pre-processing step to facilitate further processing. The method is based on the additive operator splitting (AOS) scheme [13] that allows the separation of variables. In addition, it is possible with the AOS to determine which terms and parameters in the equation are critical to the success of the solution, by examining simpler calculations on one-dimensional selected slices of the image. By tuning the parameters we obtain an inexpensive algorithm to deblur and denoise color images in one large time step.

7 References

[1] M.J. Black, G. Sapiro, D. Marimont, D. Heeger, "Robust Anisotropic Diffusion," *IEEE Transactions on Image Processing*, Vol. 7, No. 3, p.421, 1998.

[2] T.F. Chan, G.H. Golub, P. Mulet, "A Nonlinear Primal-Dual Method for Total Variation-Based Image Restoration," *SIAM Journal on Scientific Computing*, Vol. 20, No. 6, p.1964, 1999.

[3] T.F. Chan, C.K. Wong, "Total Variation Blind Deconvolution," *IEEE Transactions on Image Processing*, Vol. 7, No. 3, p.370, 1998.

[4] R. Goldenberg, R. Kimmel, E. Rivlin, and M. Rudzsky, "Fast Geodesic Active Contours," *Nielsen, P. Johansen, O.F. Olsen, J. Weickert (Eds.), Scale-space theories in computer vision*, Lecture Notes in Computer Science, Vol. 1682, Springer, Berlin, 1999

[5] J.D. Hoffman, *Numerical Methods for Engineers and Scientists,* McGraw-Hill, Inc., 1992.

[6] A. Marquina, S. Osher, "Explicit Algorithms for a New Time Dependent Model Based on Level Set Motion for Nonlinear Deblurring and Noise Removal," *UCLA CAM Report 99-5*, Department of Mathematics, University of California, Los Angeles, 1999.

[7] N. Moayeri, K. Konstantinides, "An Algorithm for Blind Restoration of Blurred and Noisy Images," *Technical Report HPL-96-102*, Hewlett-Packard, 1996.

[8] P. Perona and J. Malik, "Scale-Space and Edge Detection Using Anisotropic Diffusion," *IEEE Transactions on Pattern Analysis and Machine Intelligence*, Vol. 12, No. 7, p.629, 1990.

[9] L. Rudin, S. Osher, E. Fatemi, "Nonlinear Total Variation Based Noise Removal Algorithms," *Physica D*, Vol. 60, p.259, 1992.

[10] O. Scherzer, J. Weickert, "Relations Between Regularization and Diffusion Filtering," *Journal of Mathematical Imaging and Vision*, Vol. 12, p.43-63, 2000.

[11] R. Vogel, M.E. Oman, "Fast, Robust Total Variation-Based Reconstruction of Noisy, Blurred Images," *IEEE Transactions on Image Processing*, Vol. 7, No. 6, p.813, 1998.

[12] J. Weickert, *Anisotropic Diffusion in Image Processing*, Tuebner, Stuttgart, 1998.

[13] J. Weickert, B.M. ter Haar Romeny, M. Viergever, "Efficient and Reliable Schemes for Nonlinear Diffusion Filtering," *IEEE Transactions on Image Processing*, Vol. 7, No. 3, p.398, 1998.

[14] J. Weickert, "Efficient Image Segmentation Using Partial Differential Equations and Morphology," *Technical Report 3/2000*, Computer Science Series, University of Mannheim, Germany, 2000.